Journal of Sound and Vibration 326 (2009) 780–793

Contents lists available at ScienceDirect

Journal of Sound and Vibration

journal homepage: www.elsevier.com/locate/jsvi

Nonlinear vibration absorber coupled to a nonlinear primary system: A tuning methodology

R. Viguié *, G. Kerschen

Space Structures and Systems Laboratory, Structural Dynamics Research Group, Aerospace and Mechanical Engineering Department, University of Liège, Liège, Belgium

A R T I C L E   I N F O

Article history:
Received 30 January 2009
Received in revised form
21 April 2009
Accepted 11 May 2009
Handling Editor: M.P. Cartmell
Available online 10 June 2009

A B S T R A C T

This paper addresses the problem of mitigating the vibration of nonlinear mechanical systems using nonlinear dynamical absorbers. One particular feature of the proposed absorber is that it is effective in a wide range of forcing amplitudes. A qualitative tuning methodology is developed and validated using numerical simulations.

1. Introduction

The tuned mass damper (TMD) is one popular device for passive vibration mitigation of mechanical structures. Realizing that the TMD is only effective when it is precisely tuned to the frequency of a vibration mode [1,2], the development of nonlinear vibration absorbers effective in a larger frequency range has been undertaken. The first studies date back to Roberson [3], Pipes [4] and Arnold [5] who studied the influence of a nonlinearity on the suppression bandwidth. Hunt and Nissen [6] were the first to implement a practical nonlinear damped absorber using a softening nonlinearity.

Recent developments in passive nonlinear vibration absorbers include the autoparametric vibration absorber and the nonlinear energy sink (NES). The former absorber exploits the transfer of energy between modes, and the saturation phenomenon [7]. This occurs in quadratically coupled systems subjected to primary excitation and possessing a 1:2 internal resonance. In [8], it is shown that the bandwidth of effectiveness can be increased substantially by using an array of pendulums with slightly different natural frequencies. A few guidelines for the choice of optimum parameters giving maximum bandwidth are also given. Relying on the concept of essential nonlinearity, the NES has no preferential resonant frequency, which makes it a frequency-independent absorber [9–13]. Another salient feature of an NES is its capability to realize targeted energy transfer (TET) during which energy initially induced in the primary system gets passively and irreversibly transferred to the NES. This nonlinear device is well suited for vibration mitigation of multi-degree-of-freedom (MDOF) structures, for which it can resonate virtually with and extract energy from any mode.

One potential limitation of nonlinear vibration absorbers is that their performance depends critically on the total energy present in the system or, equivalently, on the amplitude of the external forcing. This stems from the frequency–energy dependence of nonlinear oscillations, which is one typical feature of nonlinear dynamical systems. For instance, Ref. [12] reports that there exists a well-defined threshold of input energy below which no significant energy dissipation in the NES can be achieved. In this context, the main contribution of this study is to develop a nonlinear absorber that can mitigate the vibrations of a specific mode of a nonlinear primary structure in a wide range of forcing amplitudes. Based on an extension

* Corresponding author. Tel.: +32 4 3664854; fax: +32 4 3664856.
E-mail addresses: r.viguie@ulg.ac.be (R. Viguié), g.kerschen@ulg.ac.be (G. Kerschen).

0022-460X/$ - see front matter © 2009 Elsevier Ltd. All rights reserved.
doi:10.1016/j.jsv.2009.05.023

of the tuning of a TMD coupled to a linear primary system, a qualitative tuning methodology for such a nonlinear absorber is proposed in this paper.

The paper is organized as follows. Section 2 briefly recalls the TMD tuning methodology. In Section 3, a methodology for tuning a nonlinear absorber coupled to an essentially nonlinear oscillator is developed. In Section 4, this methodology is then extended to a primary system possessing both linear and nonlinear elastic terms. The conclusions of the present study are summarized in Section 5.

2. Tuned mass damper coupled to a linear oscillator

Frahm [1] was the first to introduce the TMD concept and considered a linear attachment composed of a mass and a spring coupled to a conservative linear oscillator (LO) (see Fig. 1 with $c_1 = c_2 = 0$). This absorber was found to be efficient in a narrow frequency range centered at the natural frequency of the LO. Den Hartog [2] then reported that a TMD with energy dissipation mechanisms (i.e., $c_2 \neq 0$) increases the effective bandwidth at the cost of a reduced attenuation of the resonance peak. These studies highlighted the trade-off existing between performance (attenuation efficiency related to H_∞ optimization) and robustness (bandwidth related to H_2 optimization). Interestingly enough, the tuning methodology of a TMD coupled to a dissipative linear oscillator (i.e., $c_1 \neq 0$) [14–17] or to an MDOF linear system [18] is still an active research area.

The equations related to the undamped version of the system depicted in Fig. 1 and submitted to a forced excitation, are given by

$$m_1\ddot{x}_1 + k_1x_1 + k_2(x_1 - x_2) = F\cos\omega t,$$

$$m_2\ddot{x}_2 + k_2(x_2 - x_1) = 0. \tag{1}$$

Assuming that $x_i(t) = X_i\cos(\omega t)$, the LO displacement is expressed by

$$X_1 = \frac{(k_2 - \omega^2 m_2)F}{(k_1 + k_2 - \omega^2 m_1)(k_2 - \omega^2 m_2) - k_2^2}. \tag{2}$$

If the LO is excited at its resonance frequency $\omega_1 = \sqrt{k_1/m_1}$, and knowing that the tuning condition imposes a zero displacement of the LO ($X_1 = 0$) it follows that

$$\omega_a = \sqrt{\frac{k_2}{m_2}} = \sqrt{\frac{k_1}{m_1}} = \omega_1, \tag{3}$$

where $\omega_a = \sqrt{k_2 m_2}$ is the resonant frequency of the TMD. The performance of a TMD is now examined for direct impulsive forcing of the LO. This is realized by imparting a non-zero initial velocity to the LO ($\dot{x}_1(0) \neq 0, x_1(0) = x_2(0) = \dot{x}_2(0) = 0$). The tuning condition is verified, and weak damping is introduced to induce energy dissipation. The resulting parameter values are listed in Table 1. A numerical integration of the equations of motion is performed for varying linear stiffnesses k_1 and

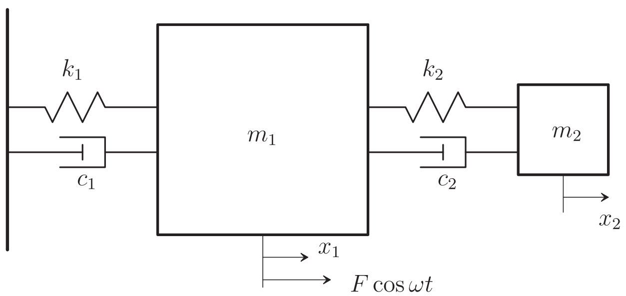

Fig. 1. Tuned mass damper coupled to a linear oscillator.

Table 1
System parameters used during the numerical simulation.

Parameter	Units	Value
m_1	kg	1
m_2	kg	0.05
c_1	N s/m	0.002
c_2	N s/m	0.002
k_1	N/m	0.5
k_2	N/m	0.025

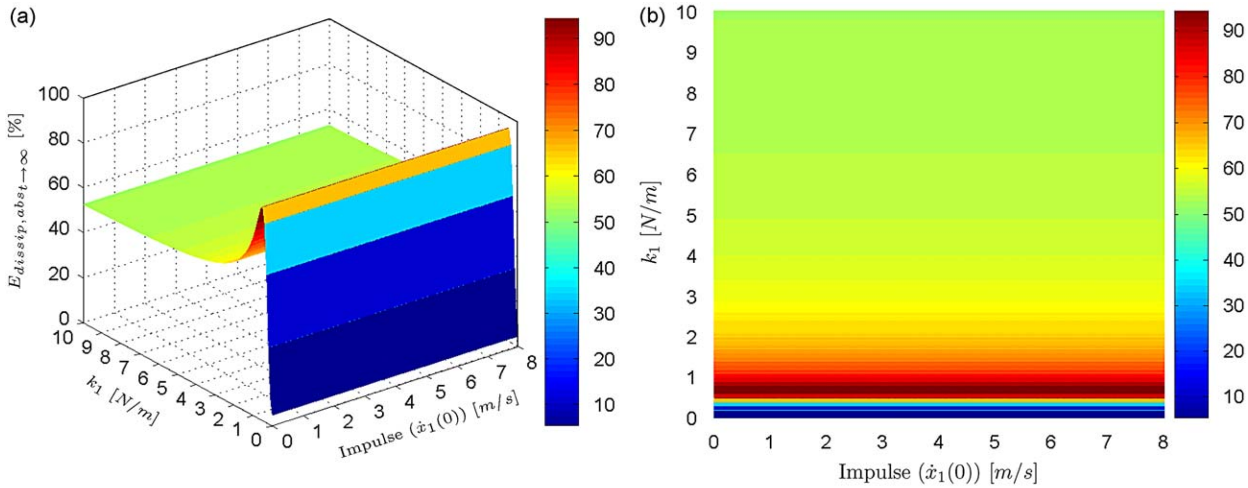

Fig. 2. Energy dissipated in the TMD against the linear stiffness of the primary system (k_1) and the impulse magnitude ($\dot{x}_1(0)$): (a) three-dimensional graph and (b) contour plot.

initial velocities $\dot{x}_1(0)$. The performance of the absorber is assessed using the ratio between the energy dissipated in the TMD and the input energy

$$E_{\text{diss,absorber,\%}}(t) = 100\frac{c_2\int_0^t(\dot{x}_1(\tau)-\dot{x}_2(\tau))^2\,d\tau}{\frac{1}{2}m_1\dot{x}_1(0)^2}. \tag{4}$$

Fig. 2 depicts this quantity against the impulse magnitude $\dot{x}_1(0)$ and the linear stiffness k_1. For $k_1 = 0.5\,\text{N/m}$ and regardless of the value of $\dot{x}_1(0)$, the TMD can dissipate a major portion of the input energy (i.e., 95 percent). However, a slight mistuning in the host structure induced by a variation of k_1 drastically reduces the TMD performance, which demonstrates its narrow effective bandwidth. The motion in the high energy dissipation region is shown in Fig. 3 for $\dot{x}_1(0) = 2\,\text{m/s}$. Clearly, the LO has a much lower response amplitude compared to the TMD, and an initial beating phenomenon visible in Fig. 3(b) is followed by a 1:1 in-phase motion of the two masses. Looking at Fig. 3(d) reveals the importance of the beating regime in the TMD performance. Strong energy exchanges occur between both oscillators and allows most of the energy initially imparted to the LO to be dissipated into the absorber.

3. Tuning of a nonlinear vibration absorber coupled to an essentially nonlinear oscillator

Although it is often overlooked by designers, nonlinearity is a frequent occurrence in engineering structures. This is why nonlinear primary structures are considered herein. Because of the frequency–energy dependence of nonlinear oscillations and of the inability of the TMD to resonate at different frequencies, our objective is to exploit nonlinearity for the design of a nonlinear vibration absorber tuned to a specific mode of a nonlinear primary system.

3.1. Basic philosophy

To progress toward this goal, appropriate tools for analyzing nonlinear oscillations, such as a frequency–energy plot (FEP) [12], have to be utilized. Periodic motions of a nonlinear system are represented by a point in the FEP, which is drawn at a frequency corresponding to the minimal period of the periodic motion and at an energy equal to the conserved total energy during the motion. A branch, represented by a solid line, is a family of periodic motions possessing the same qualitative features.

For linear systems, an FEP is not useful, because their oscillations do not exhibit any frequency–energy dependence. However, in the present study, it is interesting to see how the tuning condition (3) of a TMD coupled to an LO can be translated to the FEP concept. Fig. 4(a,b) depict the FEP of the LO and of the TMD, respectively, and show that the two FEPs are identical. In other words, the frequency of both oscillators remain the same regardless of the total energy in the system.

With the aim of mitigating the vibrations of a nonlinear system, this study is an attempt to determine a suitable configuration for a nonlinear vibration absorber. The proposed approach is to follow the tuning procedure of the TMD:

> The nonlinear absorber should possess a frequency–energy plot identical to that of the nonlinear primary system of interest.

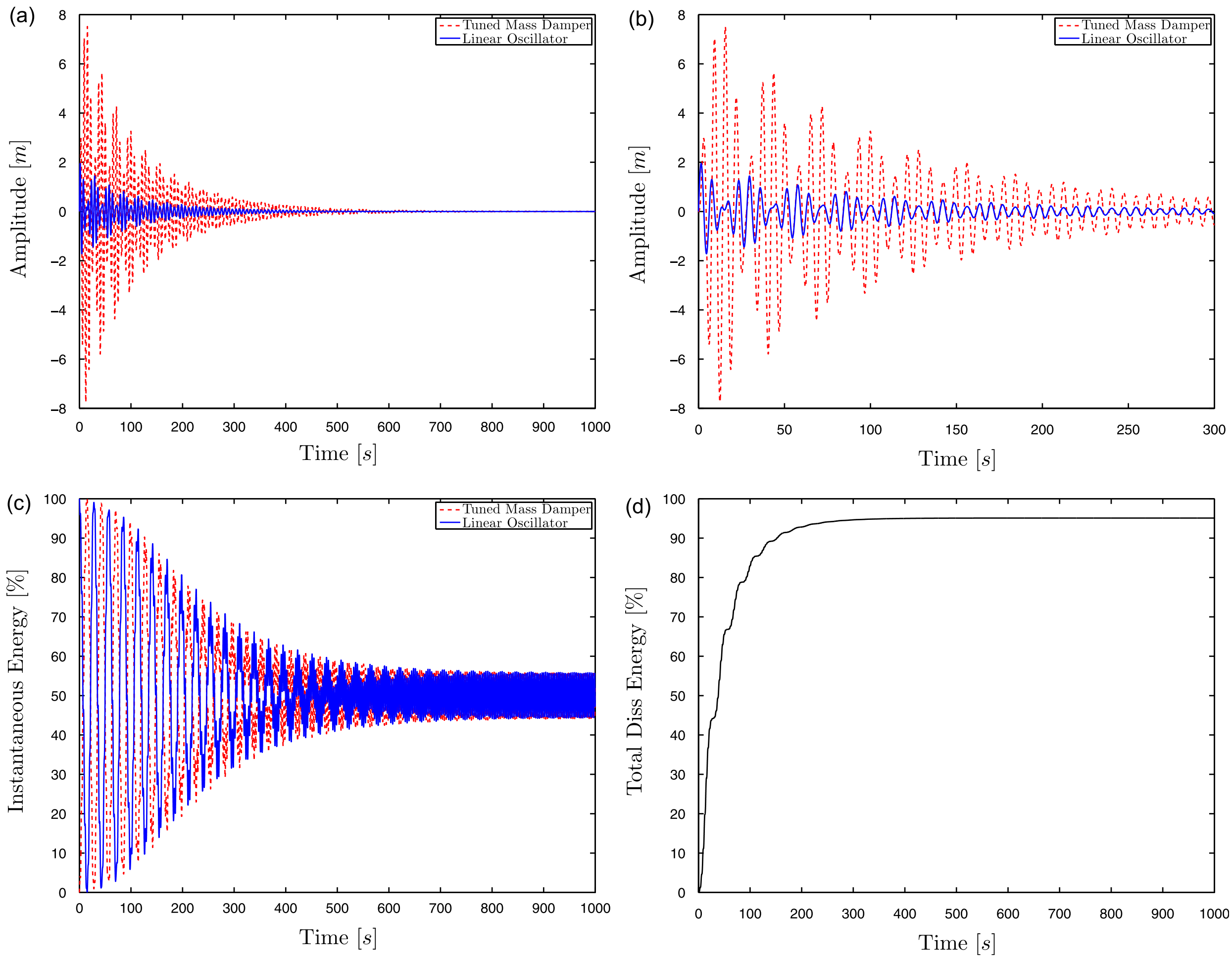

Fig. 3. Dynamics of the TMD coupled to a LO: (a) displacement responses; (b) close-up for early-time responses; (c) percentage of instantaneous total energy in both oscillators and (d) percentage of total energy dissipated in the absorber.

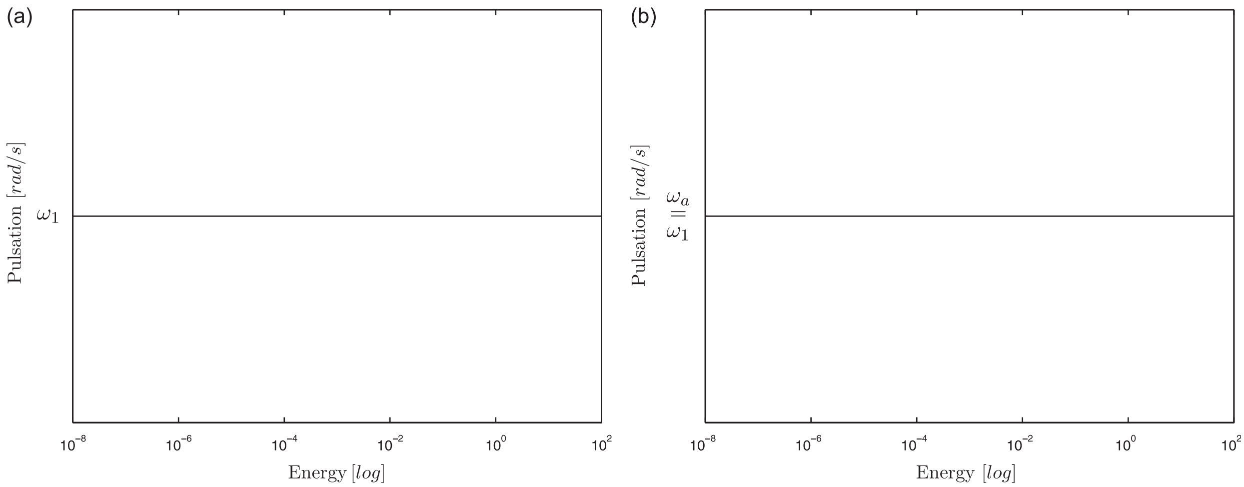

Fig. 4. Frequency–energy plots relating to (3): (a) LO and (b) TMD.

For SDOF primary systems, this can only be fulfilled if the restoring forces of the absorber and of the primary system have the same functional form. For MDOF primary systems, the absorber can only be tuned to a specific (nonlinear) mode of the host structure, because different modes will possess backbones with different frequency–energy dependence [19].

3.2. Computation of the parameters of the nonlinear absorber

For illustration, an essentially nonlinear oscillator composed of a mass m_1 and a cubic stiffness k_{nl_1} is first considered [Fig. 5(a)]. Its backbone branch is represented in the FEP of Fig. 5(b), which highlights the intrinsic frequency–energy dependence. The absence of linear stiffness in the system explains why the resonance frequency tends to zero for decreasing energy levels.

Analytical computation: According to the proposed tuning methodology, the absorber should only possess a cubic nonlinearity. The equation of motion of the resulting absorber is

$$m_2\ddot{x}_2 + k_{nl_2}x_2^3 = 0. \tag{5}$$

To compute adequate values for the mass m_2 and cubic stiffness k_{nl_2}, the harmonic balance method [20] is applied. Starting from

$$m_i\ddot{x}_i + k_{nl_i}x_i^3 = 0 \tag{6}$$

the *ansatz* $x_i(t) = A_i \cos \omega t$ is considered. Averaging over the fundamental frequency and discarding the trivial solution recasts Eq. (6) into

$$\tfrac{3}{4}k_{nl_i}A_i^2 - \omega^2 m_i = 0. \tag{7}$$

The resulting solutions highlight the frequency–amplitude dependence

$$A_{i_{2,3}} = \pm\sqrt{\frac{4\omega^2 m_i}{3k_{nl_i}}}. \tag{8}$$

At $t = 0$, $x_i(0) = A_i$, and the total energy in the system is the potential energy stored in the cubic spring

$$E_i(\omega)|_{t=0} = \frac{1}{4}k_{nl_i}A_i^4 = \frac{4m_i^2}{9k_{nl_i}}\omega^4. \tag{9}$$

The tuning condition imposes $E_1(\omega) = E_2(\omega)$ and yields

$$\frac{m_2^2}{k_{nl_2}} = \frac{m_1^2}{k_{nl_1}} \Rightarrow k_{nl_2} = \frac{m_2^2 k_{nl_1}}{m_1^2}. \tag{10}$$

Numerical computation: The problem can also be solved directly using numerical algorithms:

$$\begin{cases} x_2(t = T_i, x_2(t = 0), m_2, k_{nl_2}) - x_2(t = 0) = 0, \\ \tfrac{1}{4}k_{nl_2}x_2^4(T_i) - E_{\text{Prim}}(\omega_i) = 0, \quad i = 1, \ldots, n. \end{cases} \tag{11}$$

The first condition is a periodicity condition; i.e., periodic motions of the absorber are sought. The second condition expresses that the FEPs of the absorber and of the primary system must be identical. This problem can be solved using the combination of shooting and optimization algorithms, which, in turn, determine the absorber parameters (m_2, k_{nl_2}). This

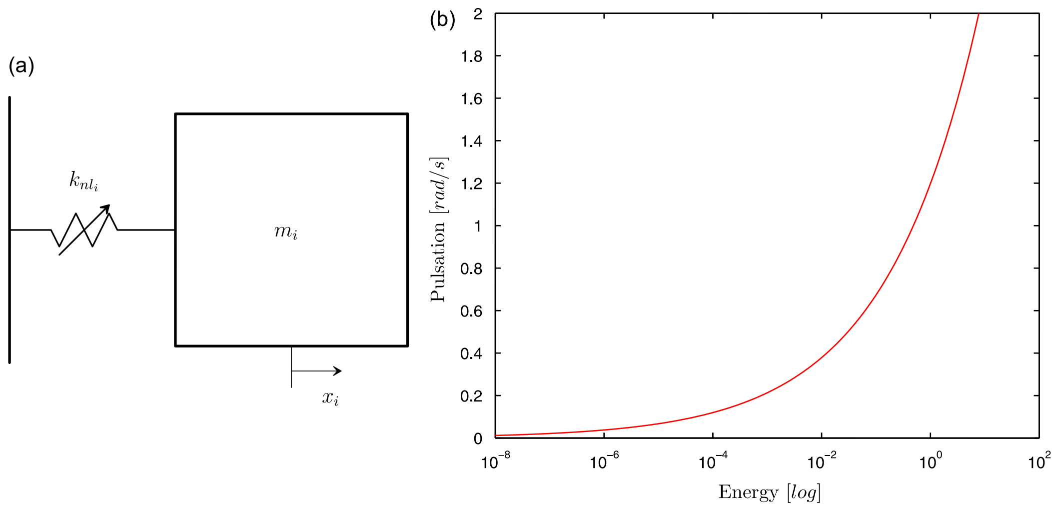

Fig. 5. (a) Essentially nonlinear oscillator and (b) FEP for $m_1 = 1$ kg and $k_{nl_1} = 1\,\text{N/m}^3$.

procedure gives accurate results, but the optimization algorithm is fairly sensitive to the initial guess (non-convex problem).

3.3. Results

The impulsive response of the coupled system depicted in Fig. 6 is now analyzed. The equations of motion are

$$m_1\ddot{x}_1 + c_1\dot{x}_1 + c_2(\dot{x}_1 - \dot{x}_2) + k_{nl_1}x_1^3 + k_{nl_2}(x_1 - x_2)^3 = 0,$$

$$m_2\ddot{x}_2 + c_2(\dot{x}_2 - \dot{x}_1) + k_{nl_2}(x_2 - x_1)^3 = 0. \tag{12}$$

The parameters of the primary system are $m_1 = 1\,\text{kg}$ and $k_{nl_1} = 1\,\text{N/m}^3$. For obvious practical reasons, a light-weight absorber is adopted, $m_2 = 0.05\,\text{kg}$. The nonlinear stiffness of the absorber is computed according to relation (10), and $k_{nl_2} = 0.0025\,\text{N/m}^3$. Weak damping $c_1 = c_2 = 0.002\,\text{N s/m}$ is also introduced to induce energy dissipation.

The performance of the nonlinear tuned absorber is examined by numerically integrating the equations of motion (12). A three-dimensional plot showing the energy dissipated in the absorber against the nonlinear stiffness k_{nl_1} and the impulse magnitude $\dot{x}_1(0)$ is displayed in Fig. 7. Interestingly, this figure bears a strong resemblance with Fig. 2, which corresponds to a TMD coupled to an LO. For $k_{nl_1} \approx 0.3\,\text{N/m}^3$ and regardless of the value of $\dot{x}_1(0)$, the tuned nonlinear absorber can dissipate a major portion of the input energy (i.e., 95 percent). In addition, the region of high energy dissipation is not localized to a particular value of k_{nl_1}, but it extends over the interval $k_{nl_1} = 0.1-0.35\,\text{N/m}^3$.

These results seem to validate the proposed tuning procedure, at least qualitatively: a nonlinear absorber that can mitigate the vibrations of a nonlinear primary structure in a wide range of forcing amplitudes has been obtained. The quantitative agreement is less convincing, because the high dissipation energy appears around $k_{nl_1} = 0.3\,\text{N/m}^3$ and not around $k_{nl_1} = 1\,\text{N/m}^3$. If the nonlinear stiffness is fixed at $k_{nl_2} = 0.0075\,\text{N/m}^3$ instead of $k_{nl_2} = 0.0025\,\text{N/m}^3$, the high dissipation energy appears around $k_{nl_1} = 1\,\text{N/m}^3$, as shown in Fig. 8. This is one limitation of the procedure, which results from the fact that the coupled system is not addressed directly. Instead the two oscillators are considered separately during the tuning.

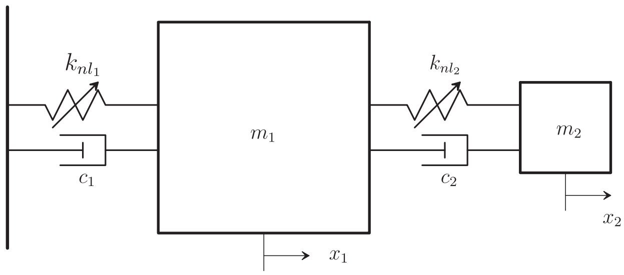

Fig. 6. Essentially nonlinear absorber coupled to an essentially nonlinear oscillator.

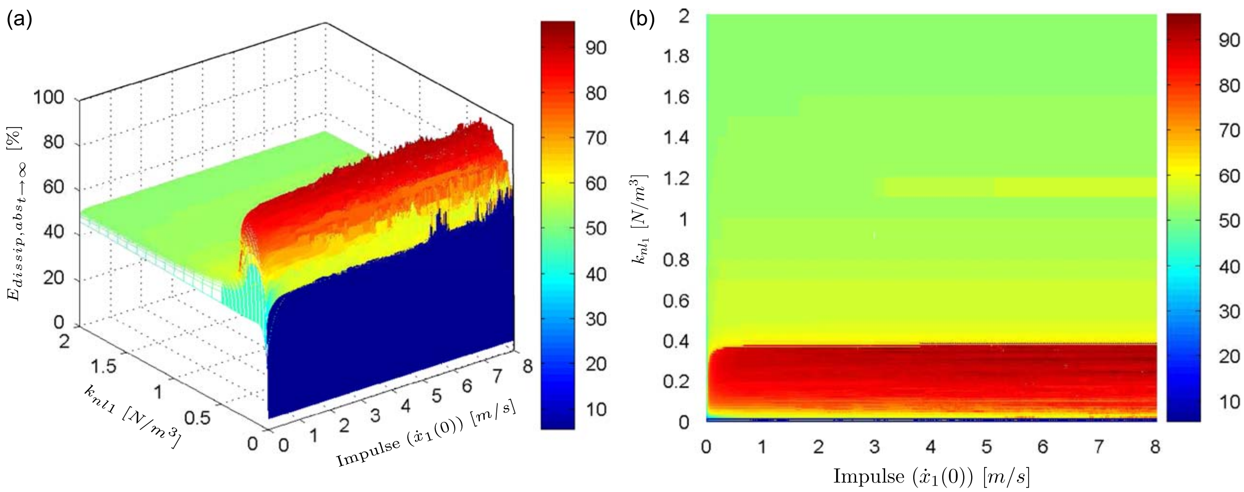

Fig. 7. Energy dissipated in the tuned nonlinear absorber (with $k_{nl_2} = 0.0025\,\text{N/m}^3$) against the nonlinear stiffness k_{nl_1} of the primary system and the impulse magnitude $\dot{x}_1(0)$: (a) three-dimensional graph and (b) contour plot.

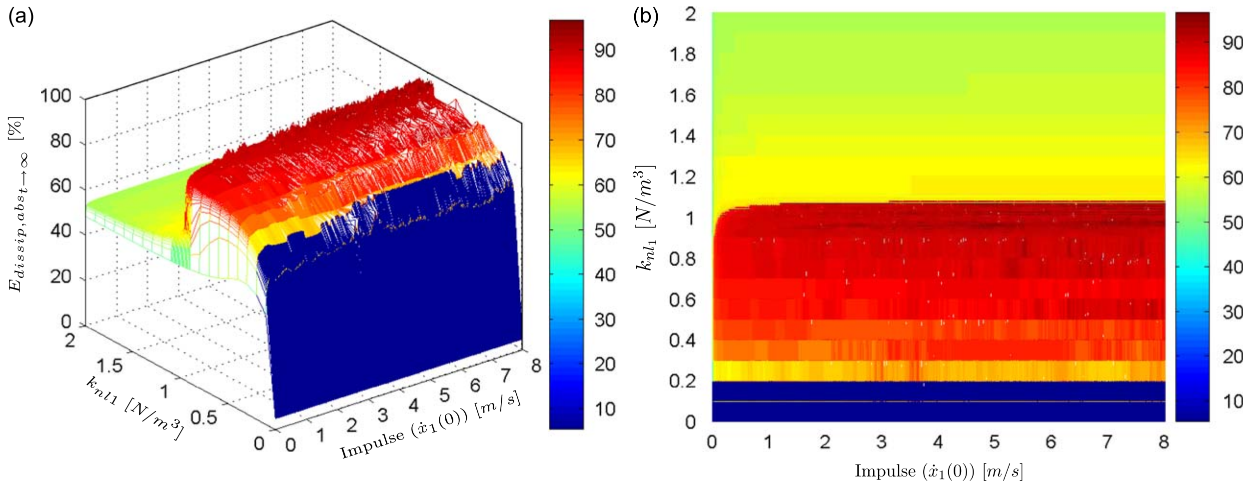

Fig. 8. Energy dissipated in the tuned nonlinear absorber (with $k_{nl_2} = 0.0075\,\mathrm{N/m^3}$) against the nonlinear stiffness (k_{nl_1}) of the primary system and the impulse magnitude ($\dot{x}_1(0)$): (a) three-dimensional graph and (b) contour plot.

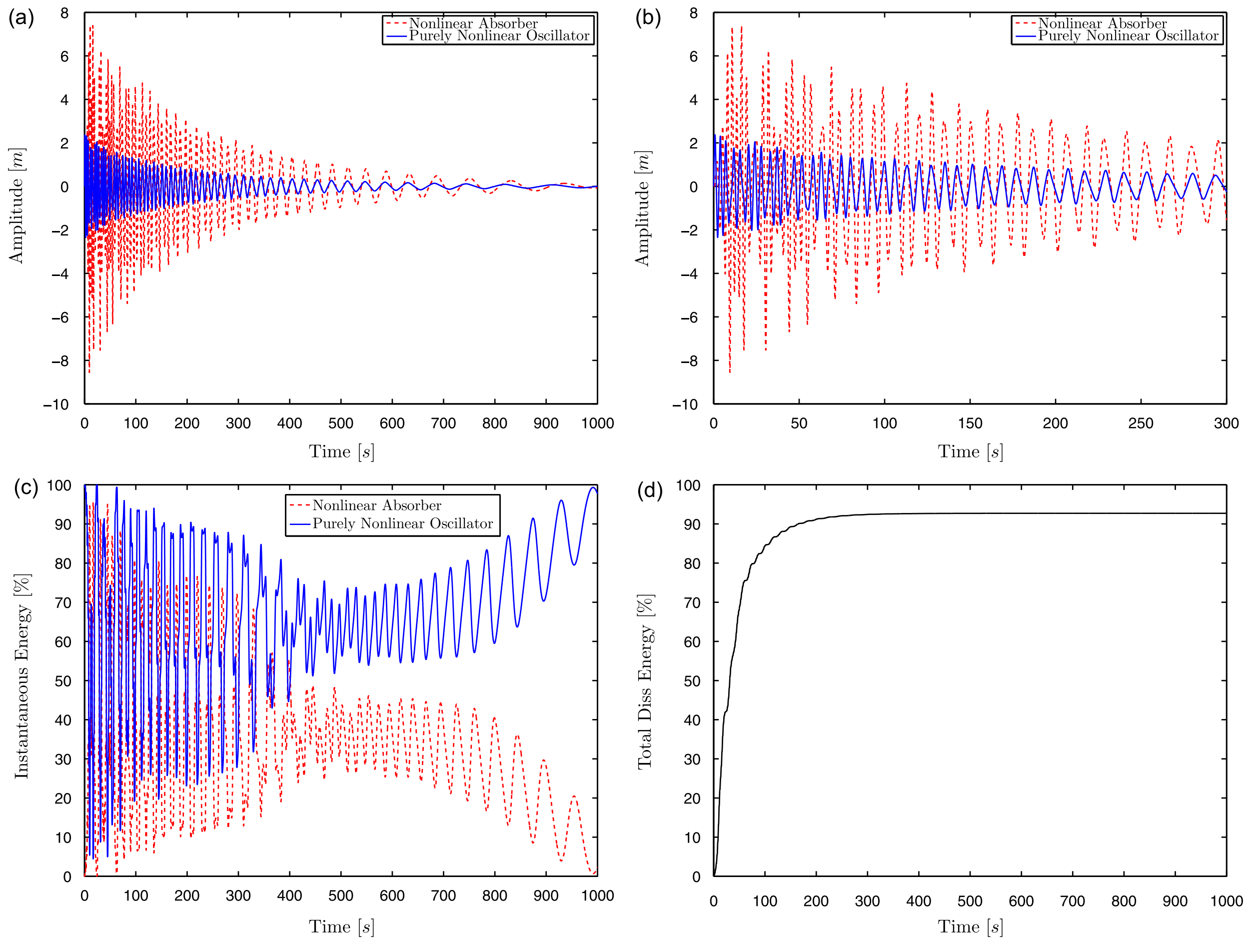

Fig. 9. Dynamics of the tuned nonlinear absorber coupled to a essentially nonlinear oscillator. (a) Displacement responses; (b) close-up for early-time responses; (c) percentage of instantaneous total energy in both oscillators and (d) percentage of total energy dissipated in the absorber.

3.4. Further analysis of the coupled system

The motion in the high energy dissipation region is shown in Fig. 9 for $k_{nl_2} = 0.0075\,\mathrm{N/m^3}$ and $\dot{x}_1(0) = 4\,\mathrm{m/s}$. The mechanisms giving rise to energy dissipation are similar to those observed for a TMD coupled to an LO in Fig. 3, namely a 1:1 in-phase motion follows the initial nonlinear beating phenomenon.

An interesting feature of the coupled system is that it possesses similar normal modes, i.e., energy-invariant straight modal curves [21]. To verify this conjecture, the condition

$$x_2(t) = \alpha x_1(t) \tag{13}$$

is imposed where α is a scalar. Plugging (13) in the conservative form of Eq. (12) and considering $\varepsilon = m_2/m_1$ yields

$$x_1^3[k_{nl_1}\varepsilon\alpha + k_{nl_2}(1-\alpha)^3(\varepsilon\alpha + 1)] = 0. \tag{14}$$

Assuming that $x_1 \neq 0$, Eq. (14) is solved with respect to the absorber nonlinear stiffness k_{nl_2}:

$$k_{nl_2} = \frac{-k_{nl_1}\varepsilon\alpha}{(1-\alpha)^3(\varepsilon\alpha + 1)}. \tag{15}$$

Because k_{nl_2} is positive, the solution is given by

$$\begin{cases} k_{nl_2} \in]0, +\infty[, \\ \alpha \in \left[-\dfrac{1}{\varepsilon}, 0\right[\bigcup [1, +\infty[. \end{cases} \tag{16}$$

We arrive to the interesting conclusion that

> Despite the fact that it has no linear springs, the coupled 2DOF system possesses straight modal lines (i.e., similar NNMs), as for linear systems.

In summary, the previous developments support that the addition of an essentially nonlinear absorber to an essentially nonlinear primary system makes the coupled system behave in a 'somewhat linear' fashion, and this despite its strongly nonlinear character.

4. Tuning of a nonlinear vibration absorber coupled to a nonlinear oscillator

The tuning methodology of the previous section is extended to nonlinear primary systems comprising both linear and nonlinear springs [Fig. 10(a)]. This system may equally well represent the motion of one specific nonlinear mode of an MDOF primary system. The frequency–energy dependence of this system is shown in the FEP of Fig. 10(b) for the parameters listed in Table 2. At low energy level, the dynamics is governed by the underlying linear system, and the oscillator exhibits a constant resonant frequency at $\omega = 1\,\mathrm{rad/s}$. For increasing energy levels, the nonlinear character of the motion becomes dominant, and the resonant frequency increases.

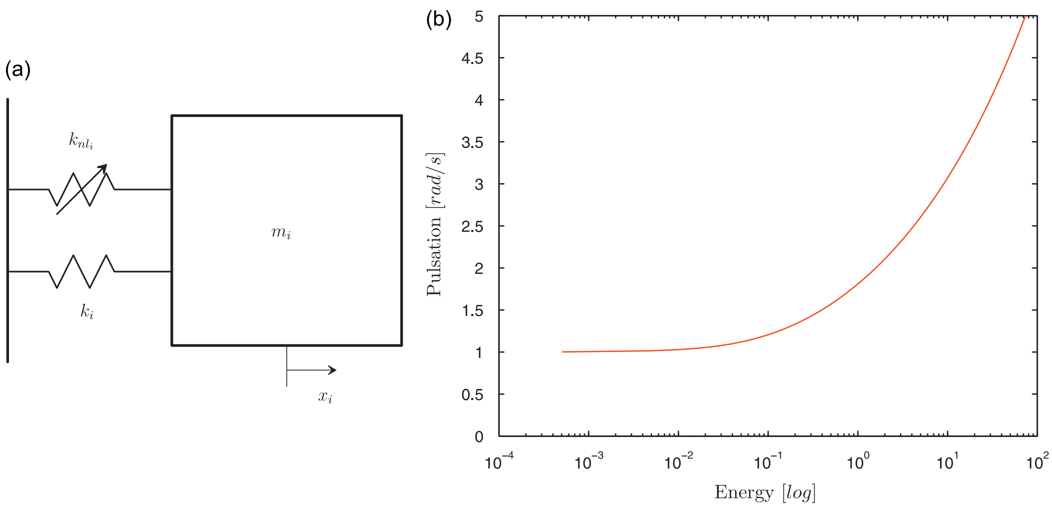

Fig. 10. Duffing oscillator: (a) configuration and (b) FEP.

Table 2
Parameters of the Duffing oscillator.

Parameter	Units	Value
m_1	kg	1
k_{nl_1}	N/m^3	4
k_1	N/m	1

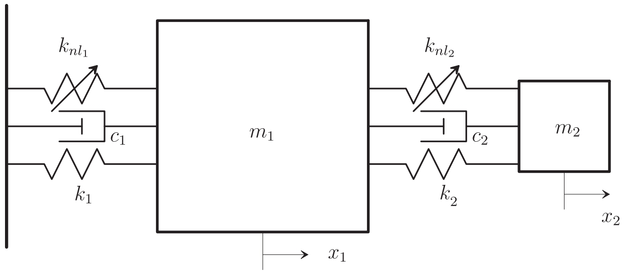

Fig. 11. Nonlinear vibration absorber coupled to a nonlinear oscillator.

4.1. Computation of the parameters of the nonlinear absorber

Analytical computation: The equation of motion of the Duffing oscillator is

$$m_i\ddot{x}_i + k_i x_i + k_{nl_i} x_i^3 = 0. \tag{17}$$

A straightforward application of the harmonic balance method gives

$$A_{i_{2,3}} = \pm\sqrt{\frac{4(\omega^2 m_i - k_i)}{3k_{nl_i}}}. \tag{18}$$

The total energy in the system is

$$E_i(\omega)|_{t=0} = \frac{1}{4}k_{nl_i}A_i^4 + \frac{1}{2}k_{nl_i}A_i^2 = \frac{4}{9k_{nl_i}}\left(m_i^2\omega^4 - \frac{1}{2}k_i(m_i\omega^2 + k_i)\right). \tag{19}$$

The tuning methodology imposes $E_1(\omega) = E_2(\omega)$, which results in

$$\frac{m_1^2}{k_{nl_1}} = \frac{m_2^2}{k_{nl_2}}, \quad \frac{k_1 m_1}{k_{nl_1}} = \frac{k_2 m_2}{k_{nl_2}}, \tag{20}$$

which can be recast into

$$\frac{k_1}{m_1} = \frac{k_2}{m_2}, \quad \frac{m_1^2}{k_{nl_1}} = \frac{m_2^2}{k_{nl_2}}. \tag{21}$$

The first and second conditions are related to the tuning condition of a TMD coupled to a LO (see Section 2) and of an essentially nonlinear absorber coupled to an essentially nonlinear oscillator (see Section 3), respectively. Therefore, the tuning of the linear and nonlinear springs of the absorber can be performed by separating explicitly the linear and nonlinear behaviors.

Numerical computation: The problem consists in solving the following system of equations:

$$\begin{cases} x_2(t = T_i, x_2(t=0), m_2, k_2, k_{nl_2}) - x_2(t=0) = 0, \\ \frac{1}{4}k_{nl_2}x_2^4(T_i) + \frac{1}{2}k_2 x_2^2(T_i) - E_{\text{Prim}}(\omega_i) = 0, \quad i = 1, \ldots, n. \end{cases} \tag{22}$$

4.2. Results

The impulsive response of the coupled system

$$m_1\ddot{x}_1 + c_1\dot{x}_1 + c_2(\dot{x}_1 - \dot{x}_2) + k_1x_1 + k_{nl_1}x_1^3 + k_{nl_2}(x_1 - x_2)^3 + k_2(x_1 - x_2) = 0,$$

$$m_2\ddot{x}_2 + c_2(\dot{x}_2 - \dot{x}_1) + k_2(x_2 - x_1) + k_{nl_2}(x_2 - x_1)^3 = 0 \tag{23}$$

is now analyzed (Fig. 11). The system parameters are given in Table 3 where the absorber mass is small, and the other absorber parameters have been chosen according to Eq. (21). Weak damping ($c_1 = c_2 = 0.002\,\mathrm{N\,s/m}$) is also introduced in both oscillators.

A three-dimensional plot of the energy dissipated in the absorber against the nonlinear stiffness k_{nl_1} and the impulse magnitude $\dot{x}_1(0)$ is numerically computed and illustrated in Fig. 12. For small excitation amplitudes ($\dot{x}_1(0) < 0.4\,\mathrm{m/s}$), the

Table 3
Parameter values of the conservative 2DOF system.

Parameter	Units	Value
m_1	kg	1
k_{nl_1}	N/m^3	4
k_1	N/m	1
m_2	kg	0.05
k_{nl_2}	N/m^3	0.01
k_2	N/m	0.05

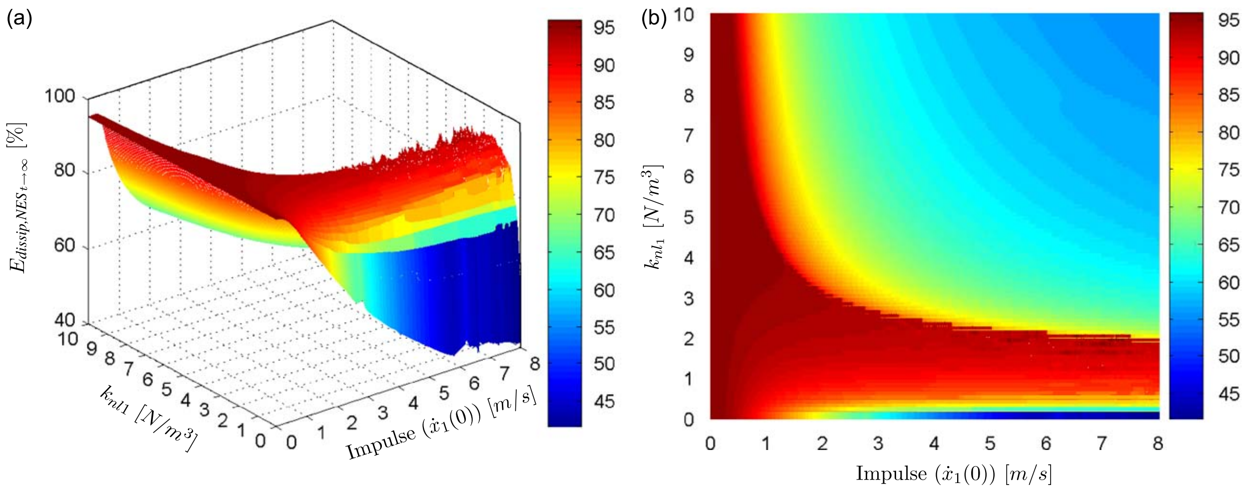

Fig. 12. Energy dissipated in the tuned nonlinear absorber for $k_{nl_2} = 0.01\,\mathrm{N/m^3}$ against the nonlinear stiffness k_{nl_1} of the primary system and the impulse magnitude $\dot{x}_1(0)$: (a) three-dimensional graph and (b) contour plot.

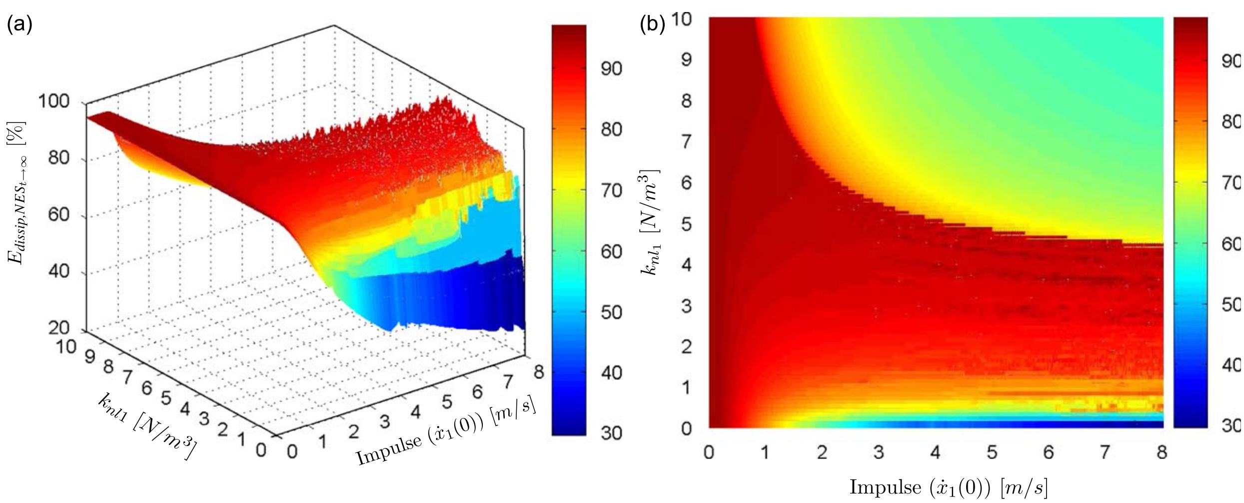

Fig. 13. Energy dissipated in the tuned nonlinear absorber for $k_{nl_2} = 0.025\,\mathrm{N/m^3}$ against the nonlinear stiffness k_{nl_1} of the primary system and the impulse magnitude $\dot{x}_1(0)$: (a) three-dimensional graph and (b) contour plot.

nonlinear springs have no influence on the dynamics of the system, which resembles that of an LO coupled to a TMD. The resulting linear dynamics explains the presence of a high energy dissipation region regardless of the value of k_{nl_1}. For increasing excitation amplitudes ($\dot{x}_1(0) > 0.4\,\mathrm{m/s}$), the nonlinear springs participate in the system dynamics to a large

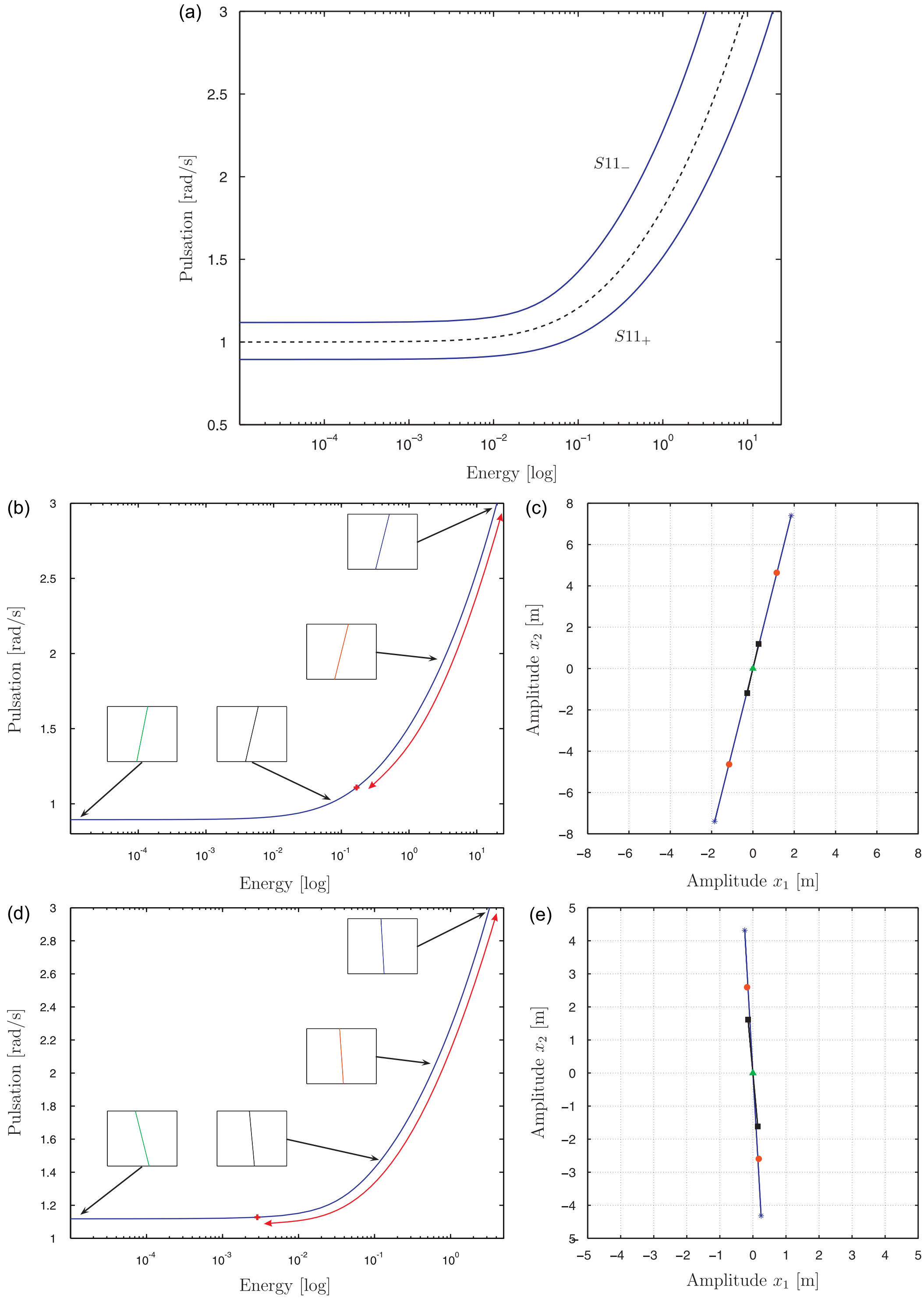

Fig. 14. Tuned nonlinear absorber coupled to a nonlinear oscillator. (a) Solid (blue) line: FEP of the coupled system; dashed (black) line: FEP of the nonlinear primary system; (b), (d) close-up of branches $S11_+$ and $S11_-$, respectively; (c), (e) motion in the configuration space for $S11_+$ and $S11_-$ branches, respectively. The red arrow in (b) and (d) represents the locus of unstable periodic motions. (For interpretation of the references to color in this figure legend, the reader is referred to the web version of this article.)

extent. At high energy levels, the system dynamics resembles that of an essentially nonlinear absorber coupled to an essentially nonlinear oscillator.

As in Section 3, these results validate the proposed tuning procedure in the sense that the effectiveness of the nonlinear absorber is not affected by the total energy present in the system. As was observed in Section 3, the quantitative agreement is questionable, because the nominal value of the nonlinear stiffness of the primary structure, $k_{nl_1} = 4\,\text{N/m}^3$, is not included in the region of high energy dissipation. To do so, k_{nl_2} has to be changed to $0.025\,\text{N/m}^3$ (Fig. 13). In this figure, we note that the high energy dissipation region is not localized to a specific value of k_{nl_1}, which shows that the absorber is robust against mistuning.

4.3. Further analysis of the coupled system

The FEP of the coupled system is depicted in Fig. 14(a) for the parameters listed in Table 3. Similarly to what is observed in the FRF of a TMD coupled to an LO, two branches of fundamental resonance $S11_+$ and $S11_-$ (blue solid lines) appear in

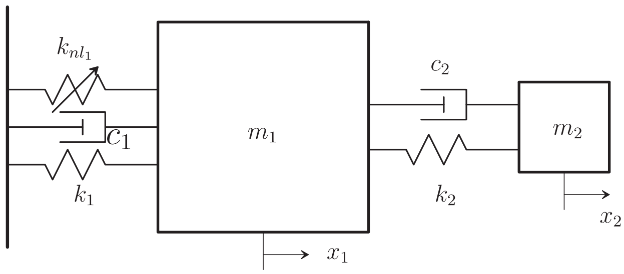

Fig. 15. Duffing oscillator coupled to a TMD.

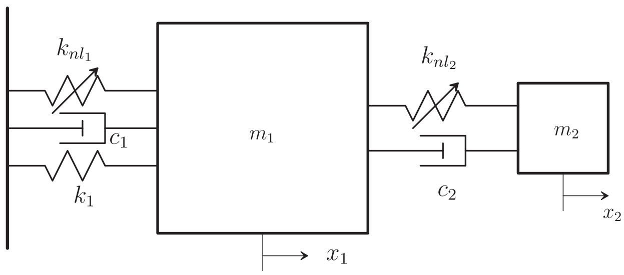

Fig. 16. Duffing oscillator coupled to an NES.

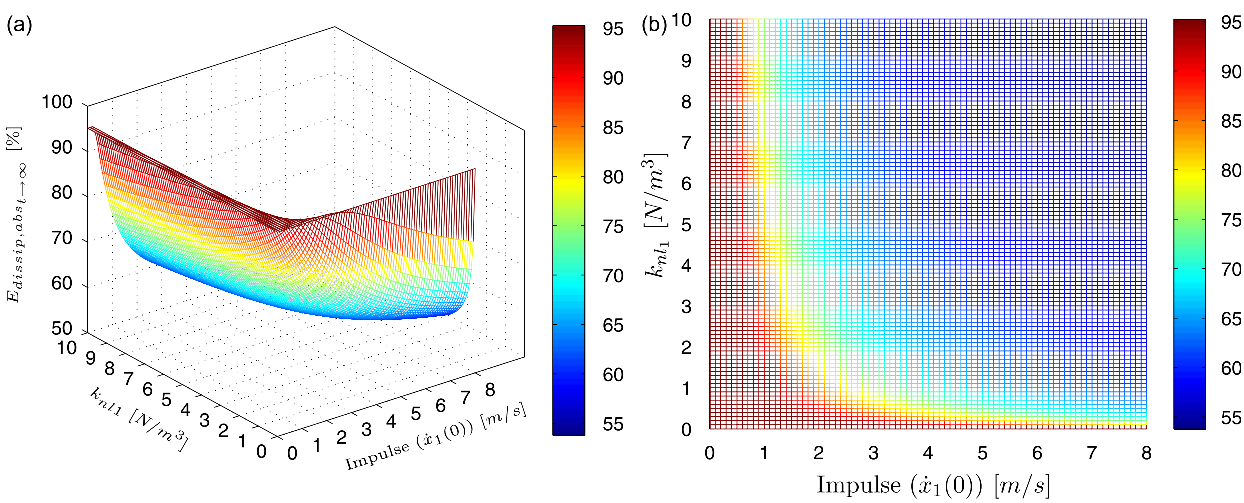

Fig. 17. TMD ($m_2 = 0.05\,\text{kg}$ and $k_2 = 0.05\,\text{N/m}$) performances when coupled to a general nonlinear oscillator. (a) Energy dissipated in the nonlinear absorber against the nonlinear stiffness of the primary system (k_{nl_1}) and the impulse magnitude ($\dot{x}_1(0)$) and (b) contour plot.

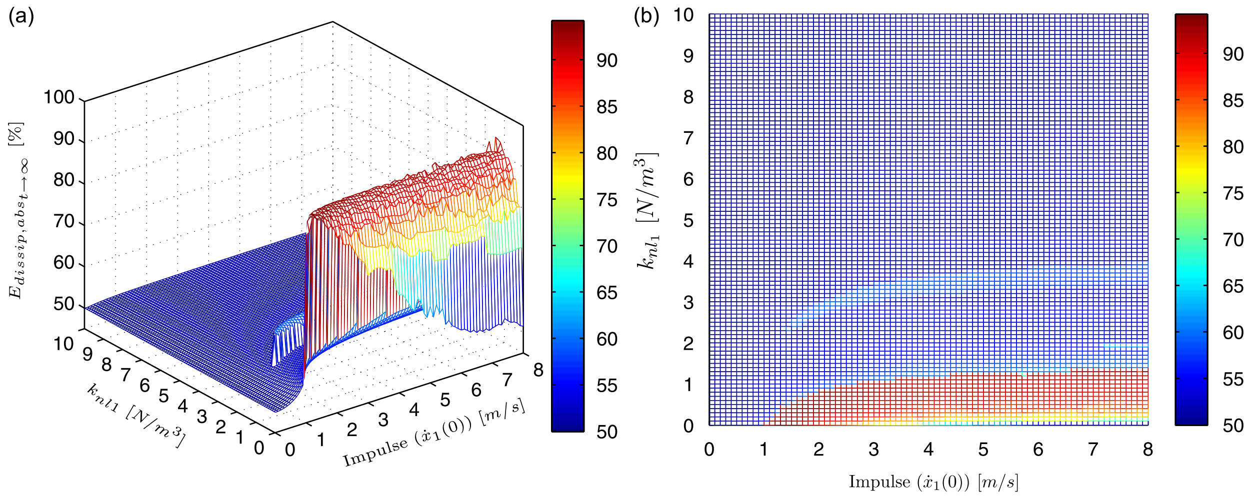

Fig. 18. Purely nonlinear absorber ($m_2 = 0.05\,\text{kg}$ and $k_{nl_2} = 0.01\,\text{N/m}^3$) performances when coupled to a general nonlinear oscillator. (a) Energy dissipated in the nonlinear absorber against the nonlinear stiffness of the primary system (k_{nl_1}) and the impulse magnitude ($\dot{x}_1(0)$) and (b) contour plot.

the vicinity of the backbone of the nonlinear primary system (black dashed line). A close-up of each branch is depicted in Fig. 14(b)–(d). The representation of the periodic motions in the configuration space in Fig. 14(c, e) shows a slight evolution of the periodic motions with energy. Unlike what was observed in Section 3.4, the modal shapes are no longer similar. Regarding the energy dissipation mechanisms, a 1:1 in-phase motion follows an initial nonlinear beating, as in the previous sections.

To further validate the proposed tuning methodology, a TMD and an essentially nonlinear absorber are coupled separately to the nonlinear primary system (see Figs. 15 and 16). Their tuning is achieved with respect to the linear and nonlinear springs of the primary system, respectively. The plots of energy dissipation are shown in Figs. 17 and 18. It can be seen that the TMD is always effective at low energy levels ($\dot{x}_1(0) < 0.5\,\text{m/s}$), but its efficiency decreases as nonlinear effects come into play. Conversely, there exists a well-defined threshold of input energy below which no significant energy dissipation in the essentially nonlinear absorber can be achieved.

5. Conclusions

Realizing that the performance of nonlinear vibration absorbers depends on the amplitude of the external forcing, this study examines a nonlinear absorber that is effective in a wide range of forcing amplitudes. A qualitative tuning methodology, which imposes the frequency–energy dependence of the absorber to be identical to that of the nonlinear primary system, is developed. The proposed absorber proves useful for mitigating the impulsive response of an SDOF nonlinear oscillator, which may also represent the vibrations of a specific mode of an MDOF primary structure.

Another finding of this study is that, despite its strongly nonlinear character, a 2DOF system comprising only essential nonlinearities seems to behave in a 'somewhat linear' fashion. For instance, this system possesses similar modes, i.e., energy-invariant straight modal curves.

Acknowledgment

The author R. Viguié would like to acknowledge the Belgian National Fund for Scientific Research (FRIA fellowship) for its financial support.

References

[1] H. Frahm, A device for damping vibrations of bodies, US Patent 989958, 1911.
[2] J.P. Den Hartog, *Mechanical Vibrations*, fourth ed., Dover Books on Engineering, 1985.
[3] R. Roberson, Synthesis of a nonlinear dynamic vibration absorber, *Journal of the Franklin Institute* 254 (1952) 205–220.
[4] L. Pipes, Analysis of a nonlinear dynamic vibration absorber, *Journal of Applied Mechanics* 20 (1953) 515–518.
[5] F. Arnold, Steady-state behavior of systems provided with nonlinear dynamic vibration absorbers, *Journal of Applied Mechanics* 22 (1955) 487–492.
[6] J. Hunt, J.-C. Nissen, The broadband dynamic vibration absorber, *Journal of Sound and Vibration* 83 (1982) 573–578.
[7] R.S. Haxton, A.D.S. Barr, The autoparametric vibration absorber, *Journal of Engineering for Industry—Transactions of the ASME* 94 (1972) 119–125.
[8] A. Vyas, A.K. Bajaj, Dynamics of autoparametric vibration absorbers using multiple pendulums, *Journal of Sound and Vibration* 246 (2001) 115–135.
[9] O.V. Gendelman, Transition of energy to a nonlinear localized mode in a highly asymmetric system of two oscillators, *Nonlinear Dynamics* 25 (2001) 237–253.

[10] O.V. Gendelman, L.I. Manevitch, A.F. Vakakis, R. McCloskey, Energy pumping in nonlinear mechanical oscillators: part i—dynamics of the underlying Hamiltonian systems, *Journal of Applied Mechanics* 68 (2001) 34–41.
[11] A.F. Vakakis, O.V. Gendelman, Energy pumping in nonlinear mechanical oscillators: part ii—resonance capture, *Journal of Sound and Vibration* 68 (2001) 42–48.
[12] A. Vakakis, O. Gendelman, L. Bergman, D. McFarland, G. Kerschen, Y. Lee, *Nonlinear Targeted Energy Transfer in Mechanical and Structural Systems*, Springer, Dordrecht, 2009.
[13] E. Gourdon, C. Taylor, N. Alexander, C.H. Lamarque, S. Pernot, Nonlinear energy pumping under transient forcing with strongly nonlinear coupling: theoretical and experimental results, *Journal of Sound and Vibration* 300 (2007) 522–551.
[14] T. Asami, O. Nishihara, A.M. Baz, Analytical solutions to h_{inf} and h_2 optimization of dynamic vibration absorbers attached to damped linear systems, *Journal of Vibration and Acoustics—Transactions of the ASME* 124 (2002) 284–295.
[15] O. Nishihara, T. Asami, Closed-form solutions to the exact optimizations of dynamic vibration absorbers (minimizations of the maximum amplitude magnification factors), *Journal of Vibration and Acoustics—Transactions of the ASME* 124 (2002) 576–582.
[16] T. Asami, O. Nishihara, Closed-form exact solution to h_{inf} optimization of dynamic vibration absorbers, Application to different transfer functions and damping systems, *Journal of Vibration and Acoustics—Transactions of the ASME* 125 (2003) 381–411.
[17] Y. Fujino, M. Abe, Design formulas for tuned mass damper based on a perturbation technique, *Earthquake Engineering & Structural Dynamics* 22 (1993) 833–854.
[18] M.B. Ozer, T.J. Royston, Extending Den Hartog's vibrations absorber technique to multi-degree-of-freedom systems, *Journal of Vibration and Acoustics—Transactions of the ASME* 127 (2005) 341–350.
[19] G. Kerschen, J.J. Kowtko, D.M. McFarland, L.A. Bergman, A.F. Vakakis, Theoretical and experimental study of multimodal targeted energy transfer in a system of coupled oscillators, *Nonlinear Dynamics* 47 (25) (2007) 285–309.
[20] A.H. Nayfeh, D.T. Mook, *Nonlinear Oscillations*, Wiley-Interscience, New York, 1995.
[21] A.F. Vakakis, L.I. Manevitch, Y.V. Mikhlin, V.N. Pilipchuk, A.A. Zevin, *Normal Modes and Localization in Nonlinear Systems*, Wiley, New York, 1996.